

# Fabrication of magnetic atom chips based on FePt

Y. T. Xing,<sup>1,\*</sup> I. Barb,<sup>1</sup> R. Gerritsma,<sup>1</sup> R. J. C. Spreeuw,<sup>1</sup> H. Luigjes,<sup>1</sup> Q. F. Xiao,<sup>2,†</sup> C. R  tif,<sup>2</sup> and J. B. Goedkoop<sup>1,‡</sup>

<sup>1</sup>*Van der Waals-Zeeman Institute, University of Amsterdam,  
Valckenierstraat 65, 1018 XE Amsterdam, The Netherlands<sup>§</sup>*

<sup>2</sup>*FOM-Institute of Atomic and Molecular Physics, Kruislaan 407,  
PO Box 41883, NL-1009 DB, Amsterdam, The Netherlands*

(Dated: December 17, 2021)

We describe the design and fabrication of novel all-magnetic atom chips for use in ultracold atom trapping. The considerations leading to the choice of nanocrystalline exchange coupled FePt as best material are discussed. Using stray field calculations, we designed patterns that function as magnetic atom traps. These patterns were realized by spark erosion of FePt foil and e-beam lithography of FePt film. A mirror magneto-optical trap (MMOT) was obtained using the stray field of the foil chip.

PACS numbers: 75.75.+a, 74.78.Na, 39.25.+k, 03.75.Be, 39.25.+k

## I. INTRODUCTION

The rapidly proceeding development of techniques to manipulate the motion of ultracold atoms has recently led to the invention of so-called atom chips. An atom chip is a planar structure that produces a designer magnetic field pattern in the vacuum above the structure. The magnetic field minima are used to confine atoms carrying a magnetic dipole moment  $\mu$ . The confining force results from the magnetic dipole interaction ( $-\mu \cdot \mathbf{B}$ ). An endless variety of structures can be created, including atomic wave guides, interferometers, arrays of atom traps for quantum information processing and atomic conveyor belts [1, 2]. Atom chips are now emerging as an extremely powerful and versatile tool [1, 3], and even seem to provide a simpler method to achieve Bose-Einstein condensation (BEC) [4, 5, 6]. Furthermore, atom chips allow one to reduce the time scale of trapping experiments, which could imply that the vacuum requirements can be relaxed [7].

So far, atom chips use planar patterns of current-carrying wires to generate the magnetic fields. Here we investigate a promising alternative based on hard magnetic materials patterned by micromachining or lithographic techniques [8, 9, 10, 11].

The use of hard magnetic films has many potential advantages. Firstly, since no lead wires are required, magnetic structures offer a great design flexibility, allowing for more intricate patterns including structures that are topologically impossible with current-carrying wires. Secondly, there is no resistive power dissipation, current

noise from power supplies nor stray field from lead wires. Thirdly, the conductivity of magnetic materials can be orders of magnitude lower than Cu or Au. This could help to overcome the lifetime reduction due to coupling of the cold atom cloud to random thermal currents in the chip structure [12, 13, 14]. Finally, we calculate that magnetic field gradients of  $\sim 20$  kT/m should be achievable, considerably higher than the highest values that have been achieved with current conductors.

An obvious advantage of current-conducting chips is the possibility to switch or modulate the currents. In magnetic chips the magnetic field pattern can only be manipulated by applying fields generated by external electromagnets. However, hybrid chips, combining the best parts of the two techniques, are technologically possible and will be used in future.

Currently, we are exploring the possibilities of planar magnetic structures for the confinement and manipulation of cold atoms in all-magnetic atom chips [15]. In this paper, we discuss aspects of the fabrication of such chips. In particular, we discuss the material requirements that led us to the choice of FePt as most suitable material. We give details on the fabrication of two FePt-based atom trap designs of respectively sub-millimeter and sub-micron dimensions. The first design consists of a pattern cut out of a 40  $\mu\text{m}$  thick FePt foil using spark erosion. The stray field of this structure allowed the operation of a millimeter-size magneto-optical trap for Rb atoms, thus showing the suitability of FePt as a material. The second design is an array of micron sized magnetic traps patterned in a 250 nm thick FePt film on Si using e-beam lithography techniques. We describe details on the FePt film optimization and the patterning process for this design.

## II. SELECTION OF THE HARD MAGNETIC MATERIAL

In permanent magnetic atom chips the cold atoms are statically trapped in the stray field generated by perma-

\*Present address: Centro Brasileiro de Pesquisas F  sicas (CBPF), Rua Dr. Xavier Sigaud 150, Urca Rio de Janeiro CEP 22290-180, Brazil

†Present address: Department of Physics and Astronomy, University of Victoria, Victoria, British Columbia, Canada

‡Electronic address: goedkoop@science.uva.nl

§URL: <http://www.science.uva.nl/research/aplp/>

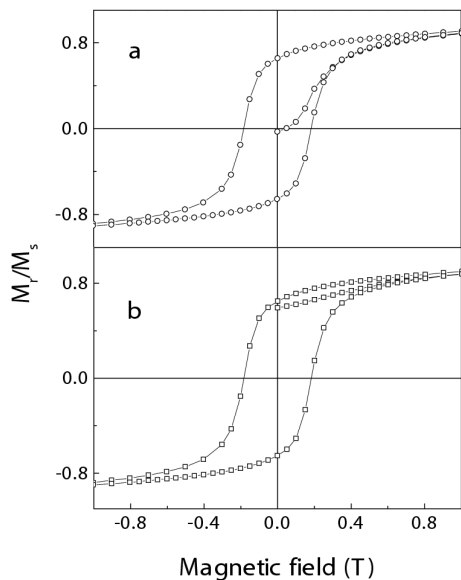


FIG. 1: Magnetization loops of a 40  $\mu\text{m}$  foil of nanocrystalline FePt with in-plane magnetization, before and after baking, (a) and (b), at 170  $^{\circ}\text{C}$  for 24 hours.

nent magnetic structures which, when properly designed, do not require external fields. The stray field determines the depth of the available atom traps which should be on the order of 0.1-1 mT.

The first material requirement is obviously a high magnetization in order to effectively generate the strong field gradients. However, each magnetic material tends to break up in domains exactly in order to reduce the stray field that it produces. This demagnetization problem is compounded by the external fields used for loading the atoms into the traps. A second requirement is therefore that the material has a high coercivity.

Since the most exciting prospect for atom chips is the possibility to integrate many microscopic atom optical devices on a single chip, the material should be suitable for preparation as a film. Clearly, the magnetic fields produced by such a thin film structure scales with its thickness. In order to produce a large enough stray field at a distance of a few  $\mu\text{m}$  from the surface with a few micron line width, the material thickness should be in the range of 100 nm to 1  $\mu\text{m}$ .

In addition, the material should be corrosion resistant in order to allow micromachining or lithographic patterning. In order to avoid uncontrolled spatial variations of the stray field, the material must also be highly homogeneous, which puts severe constraints on these manufacturing processes. Finally, the traps are operated in ultrahigh vacuum, which means that the magnetization should survive a 24 hours bake out at 150 $^{\circ}\text{C}$ .

The combination of high magnetization and high anisotropy limits the range of materials naturally to the strongest room temperature permanent magnets which are  $\text{Nd}_2\text{Fe}_{14}\text{B}$ ,  $\text{Co}_5\text{Sm}$  and FePt alloys (see e.g. [16]). Among these, the hard magnets  $\text{Co}_5\text{Sm}$  and  $\text{Nd}_2\text{Fe}_{14}\text{B}$

have excellent magnetic properties, but are difficult to grow as thin films. Moreover,  $\text{Nd}_2\text{Fe}_{14}\text{B}$  is unstable at bake out temperatures. The other candidates are the CoPt and FePt systems, where the latter has the higher magnetization and was therefore selected as the best material. FePt has been studied extensively both in bulk [17, 18] and thin film [19, 20, 21, 22, 23] form since it combines high magneto-crystalline anisotropy with high saturation magnetization  $M_s$  [16] and has excellent stability and corrosion resistance. FePt has a disordered face-centered cubic (fcc) structure at high temperature, which has a very high  $M_s$  but is magnetically soft. The low temperature equilibrium structure on the other hand is face-centered tetragonal (fct or  $\text{L}_{10}$ ), in which the Fe and Pt order in an atomic multilayered structure with stacking in the  $[111]$  direction. This phase has a lower  $M_s$  but very high magneto-crystalline anisotropy and coercivity. It has been shown that annealing of either the fcc phase obtained from the melt [24] or as-deposited thin films produces nanocrystalline composites of the two phases in which the nanocrystallites of the hard fct phase orient the surrounding soft phase by exchange coupling. This results in a material which combines high magnetization with isotropic hard magnetic behavior.

### III. FABRICATION OF AN ATOM CHIP BASED ON FePt FOIL

As a first step towards thin film chips we created a trap from FePt foil produced by bulk metallurgic techniques [24]. This method is suitable for traps with millimeter dimensions. A  $\text{Fe}_{0.6}\text{Pt}_{0.4}$  alloy was made by arc-melting in a purified Ar atmosphere. The melt was cast into a water-cooled copper mould to get cylindrical samples with a diameter of 1.5 mm. These were sealed into evacuated quartz tubes and homogenized at 1300  $^{\circ}\text{C}$  for 3 hours after which they were quenched into ice water without breaking the quartz tube to produce fct grains in an fcc matrix. Subsequently the samples were annealed for 16 minutes at 580  $^{\circ}\text{C}$  in order to obtain the nano-composite FePt.

A bar of this material was rolled into a 100  $\mu\text{m}$  thick foil and then mechanically polished to 40  $\mu\text{m}$  thickness. Figure 1a shows the in-plane magnetization loop of this material measured with SQUID. From this figure one can see that the ratio of remanent to saturation magnetization  $M_r/M_s$  is about 0.8, the reduction being due to canting of magnetization in grains which have their magnetic anisotropy directions away from the field direction. The coercivity is about 0.2 T, large compared to the external field that is applied to manipulate the atoms (10 mT). Since saturation requires at least 3 Tesla it is impossible to magnetize in-situ. It is therefore crucial that the material maintains its magnetization during the 150  $^{\circ}\text{C}$  vacuum bake-out. As figure 1b shows, the magnetization of a saturated sample that was baked at 170  $^{\circ}\text{C}$  for 24 hours decreased less than 5 %.

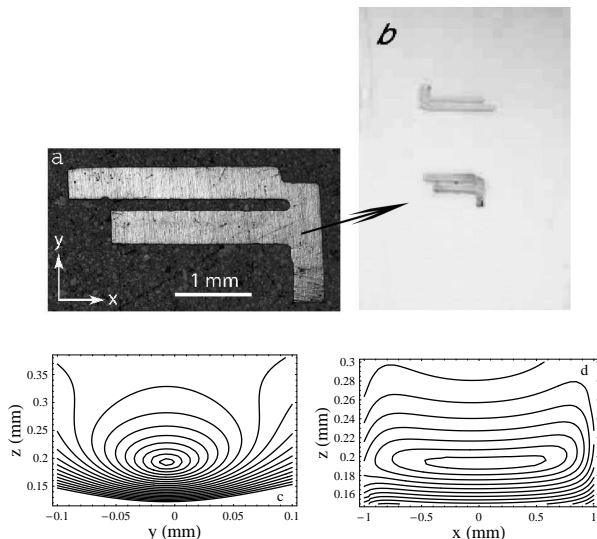


FIG. 2: (a) Foil atom chip. (b) Photograph of two FePt structures with slightly different dimensions glued on an aluminum mirror. (c)  $y$ - $z$  and (d)  $x$ - $z$  plots of the calculated magnetic stray field for the lower structure in (b). Shown are contours of equal magnitude of magnetic field  $B$  (i.e. equipotential lines), with a spacing of 6 G between the contours, in planes containing the trap minimum. The chip surface is at  $z=0.2$  mm.

CNC controlled spark erosion using a  $50\ \mu\text{m}$  wire was used to produce elongated F-like patterns (Fig. 2a). After cutting, the damaged surface layer of the outer edges of the F-shape sample was removed by mechanical polishing. Two such samples were mounted on an aluminum mirror using UHV compatible glue, as shown in Fig. 2. Finally, the samples were magnetized in a 3 Tesla field oriented along the stem of the F ( $y$ -direction) before they were put into the vacuum chamber. The two arms of this F structure form in-plane dipole magnets in the  $y,z$ -plane with the field in the short direction, which combined produce a zero field line above the gap between them. The stray field from the stem of the F has a component in the  $x$ -direction which serves to offset this minimum in order to avoid Majorana spin flips [25, 26, 27, 28].

The structure was designed as one piece to obtain sufficient mechanical precision. The smallest size of the gap between the two hands of the big F shape is determined by the diameter of the wire that we used to cut the sample. In the optimization we only used one gap size and tuned the shape and the dimensions of the pattern according to the gap size and the thickness of the foil.

The calculated stray field in the  $y, z$  and  $x, z$  planes of the F pattern of Fig. 2a are shown in Fig. 2c and 2d. The figure shows contour lines of equal magnitude of the magnetic field  $B = |\mathbf{B}|$ , which effectively acts as the potential energy for cold atoms. The calculation yields harmonic trapping frequencies in the bottom of the trap of 51 Hz and 6.8 kHz, in the longitudinal and transverse directions, respectively. The trap depth is about 11 G.

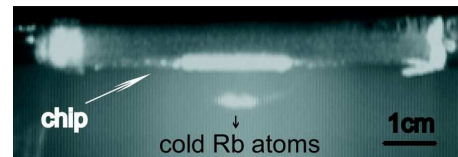


FIG. 3: Fluorescence image of a cloud of cold  $^{87}\text{Rb}$  atoms under the mirror. Mirror magneto-optical trap, using the stray field of the structure, at about 2 mm below the lower "F" shown in Fig. 2b.

The upper F pattern in Fig. 2b has calculated trapping frequencies of 34 Hz and 11 kHz and a trap depth of 33 G. More details about the trap design will be published in a separate publication [15]. Figure 3 shows the fluorescence from a cloud of  $\sim 2 \times 10^6$  cold Rb atoms trapped under this foil in a so-called mirror magneto-optic trap (MMOT), using a combination of a quadrupole magnetic field and four laser beams. It should be noted that in this case the quadrupole field is achieved by adding a 2 G external field that cancels the field of the F structure at a distance of 2 mm from the surface. This creates a point of zero magnetic field, with a gradient of  $\sim 15$  G/cm. The MMOT merely uses the decaying magnetic stray field far from the structure. True magnetic trapping has also been achieved with this structure, as described in ref. [15].

#### IV. ATOM CHIP BASED ON LITHOGRAPHICALLY PATTERNED $\text{FePt}$ FILMS

Our second sample is based on a FePt film deposited on Si. The thickest films that can be grown with vacuum deposition and that can be structured using lithographic techniques are in the micron range, implying scale reduction of a factor 40 or more with respect to the design discussed above. Here we used 250 nm  $\text{Fe}_{50}\text{Pt}_{50}$  films, co-evaporated by Molecular Beam Epitaxy (MBE) from Fe and Pt targets on rotating Si substrates at  $350\ ^\circ\text{C}$ . Details on the material optimization [29] are summarized as follows. The as-deposited samples have a strongly disordered structure, in which both fcc and fct phase are present according to X-ray diffraction. This film is post-annealed to obtain the proper characteristics. Figure 4 shows the magnetic properties of the thick film as a function of annealing temperature. From this figure one can see that the best magnetic properties (optimum  $M_r/M_s$ ) are:  $M_s=750$  kA/m,  $M_r/M_s = 0.93$ ,  $H_c = 0.83$  T for out-of-plane magnetization ( $T_{\text{anneal}}=450\ ^\circ\text{C}$ ) and  $M_r/M_s = 0.90$ ,  $H_c = 1$  T for in-plane magnetization ( $T_{\text{anneal}}=500\ ^\circ\text{C}$ ). These loops show that the magnetic properties of these films are comparable to the bulk material. A very desirable aspect of these results is that these films can be used both for in-plane and for out-of-plane chip designs. In the remainder of this section we will describe the production of an in-plane design on the basis of this film material.

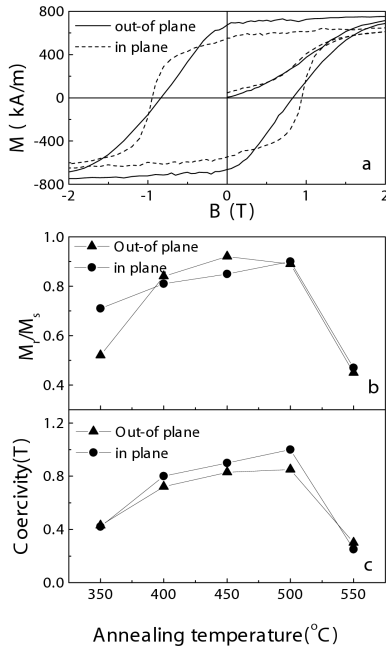


FIG. 4: Magnetic properties of the 250 nm FePt film. (a) The hysteresis loop after a 450°C anneal for 3 minutes. (b)  $M_r/M_s$  and (c) coercivity of the film as a function of temperature.

The films were patterned with e-beam lithography, using a hard negative photoresist (SU-8), to save writing time. The patterning process consists of the following steps: First the surface is roughened using Ar plasma pre-etching in order to increase the adhesion of the SU-8 on the FePt surface. After spin-coating and pre-bake a 340 nm thick SU-8 photoresist layer was obtained. The desired pattern was written in this resist using a JEOL 6460 SEM equipped with a Raith Quantum pattern generator. After writing the resist is post-baked, developed to remove the non-exposed resist and hard-baked in order to harden the remaining resist layer.

The resist structure is subsequently transferred to the FePt layer by Ar plasma etching with an Oxford Plasmalab 80 Plus reactive ion etching system. The samples were etched for 7 minutes in order to slightly over-etch the FePt layer to get very clear patterns. Figure 5a shows a typical FePt pattern and the cross section of one strip revealing a slope of the FePt edge of about  $45^\circ$ , with a roughness of about 50 nm, which is of the order of the nanocrystalline grain size.

The etching rates of the SU-8 and FePt are almost the same (40 nm/min) but the photoresist layer is thicker than FePt, and the inset shows that there is still a photoresist layer left on top of the FePt layer. It is straight forward to adjust the initial resist thickness in order to reduce this layer. Furthermore, since the final chip is coated with a thin Au film to obtain a highly reflecting surface, the thin photoresist layer has little effect.

According to the simulation, with no externally applied bias the longitudinal and transverse trapping frequencies

for the array of Fig. 5a are 691 Hz and 35 kHz, respectively. The trap depth is about 2.7 G. The structure shown here will produce traps only with in-plane magnetization. For out-of-plane magnetized samples the design must be changed accordingly. Figure 5b shows an array of identical patterns on one chip, illustrating another advantage of hard magnetic atom chips: many patterns can be made on one chip. The sample shown here will be field tested after it has been covered with a Au layer to make a mirror.

## V. DISCUSSION

The success of the foil-based MMOT as well as the magnetic trap shows that the principle of trapping using permanent magnetic materials is feasible. Further reduction of the dimensions with this technique is impossible and the future development will center on the thin film technology. The thin film design presented here will be tested in the near future. It should be noted that this design can still be improved on several points. An important issue is related to the smoothness of the structures. Fragmentation of trapped atom clouds close to a current-carrying wire has recently been attributed to edge roughness of the wires and/or defects inside the wire [30, 31]. It is to be expected that the requirements on the edge roughness of our magnetic film patterns will be similar. The edge roughness in Fig. 5 is on the order of 50 nm, which is a few percent of the width of the strip. This is much better than some of the first generation of current-carrying wire atom chips, and only slightly worse than state-of-the-art wire chips. We expect reduction of the resist layer will further reduce the roughness. An interesting alternative to lithographic patterning is to write the patterns using magneto-optic recording techniques [32] instead of lithography. This would in principle double the field gradients and make the patterning process reversible. Yet another possibility that we will investigate is the use of electrodeposition on lithographically masked ultrathin conducting substrates [33]. Finally, a promising extension of our work in the future would be to create atom chips using a combination of magnetic materials and other elements, such as current-carrying wires or electrodes for creating electrostatic potentials.

## VI. SUMMARY

We have used the magnetic properties of FePt foils and thick films to produce atom chips to trap ultra-cold atoms. FePt patterns were fabricated from 40  $\mu\text{m}$  foil using spark-erosion and from 250 nm film using e-beam lithographic patterning. The patterns generated in the FePt film have an edge roughness of about 50 nm. The foil chips were successfully used to trap cold Rb atoms, both as a mirror magneto-optic trap and as a magnetic trap. It is expected that the atom chip based

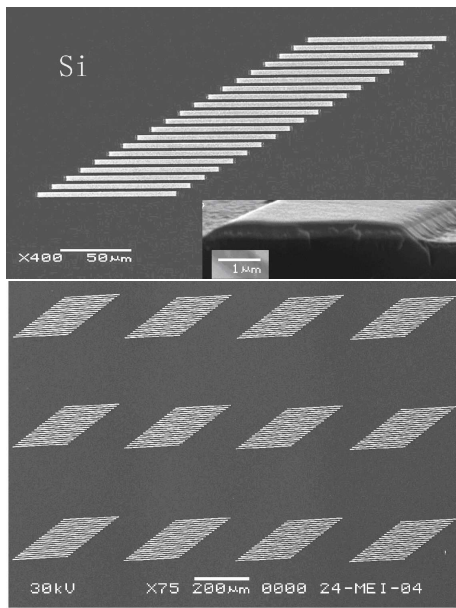


FIG. 5: (a) Patterned 250 nm FePt film on Si substrate. The inset shows the cross section of one strip of the pattern, as well as the edge roughness. The upper layer consists of SU-8 photoresist. (b) Array of strips on a single chip.

on the hard magnetic material will have certain advantages over chips based on current-carrying wires, such as the absence of perturbing lead wires, current noise, thermal noise, and power dissipation. For the two foil chips the calculated longitudinal and transverse trapping frequencies are (51 Hz, 6.8 kHz) for the first sample and (34 Hz, 11 kHz) for the second. For the film chip these frequencies are (690 Hz, 35 kHz) and (300 Hz, 36 kHz). We demonstrated that hundreds of traps can be concentrated per  $\text{mm}^2$  of chip area, with still room for further optimization. This makes the film chip a promising system for quantum information processing.

### Acknowledgments

This work was supported by Stichting Fundamenteel Onderzoek der Materie (FOM), and was made possible by the fabrication and characterization facilities of the Amsterdam nanoCenter. This work is part of the research program of the Stichting voor Fundamenteel Onderzoek van de Materie (Foundation for the Fundamental Research on Matter) and was made possible by financial support from the Nederlandse Organisatie voor Wetenschappelijk Onderzoek (Netherlands Organization for the Advancement of Research). This work was supported by the EU under contract MRTN-CT-2003-505032.

- 
- [1] R. Folman *et al.*, Adv. At. Mol. Opt. Phys. **48**, 263 (2002).
  - [2] J. Reichel, Appl. Phys. B **75**, 469 (2002).
  - [3] J. Reichel, W. Hänsel, and T. Hänsch, Phys. Rev. Lett. **83**, 3398 (1999).
  - [4] W. Hänsel, P. Hommelhoff, T. W. Hänsch, and J. Reichel, Nature **413**, 498 (2001).
  - [5] H. Ott *et al.*, Phys. Rev. Lett. **87**, 230401 (2001).
  - [6] C. D. J. Sinclair *et al.*, , arXiv:physics/0503619.
  - [7] J. Reichel, Sci. American. **32** (2005).
  - [8] J. C. Lodder, J. Magn. Magn. Mater. **272–276**, 1692 (2004).
  - [9] T. J. Davis, J. Opt. B: Quantum Semiclass. Opt. **1**, 408 (1999).
  - [10] A. Sidorov *et al.*, Acta Physica Polonica B **33**, 2137 (2002).
  - [11] C. D. J. Sinclair *et al.*, , arXiv:physics/0502073.
  - [12] C. Henkel, S. Pötting, and M. Wilkens, Appl. Phys. B **69**, 379 (1999).
  - [13] M. P. A. Jones *et al.*, Phys. Rev. Lett. **91**, 080401 (2003).
  - [14] D. Harber, J. McGuirk, J. Obrecht, and E. Cornell, J. Low Temp. Phys. **133**, 229 (2003).
  - [15] I. Barb *et al.*, (2005), DOI: 10.1140/epjd/e2005-00055-3.
  - [16] D. Weller and M. Doerner, Ann. Rev. Mat. Sc. **30**, 611 (2000).
  - [17] Q. F. Xiao *et al.*, J. All. Comp. **364**, 315 (2004).
  - [18] P. D. Thang *et al.*, IEEE Trans. Magn. **38**, 2934 (2002).
  - [19] M.-G. Kim, S.-C. Shin, and K. H. Kang, Appl. Phys. Lett. **80**, 3802 (2002).
  - [20] C. L. Platt *et al.*, J. Appl. Phys. **92**, 6104 (2002).
  - [21] M. Weisheit, L. Schultz, and S. Fähler, J. Appl. Phys. **95**, 7489 (2004).
  - [22] H. Bernas *et al.*, Phys. Rev. Lett. **91**, 077203 (2003).
  - [23] M. L. Yan, N. Powers, and D. J. Sellmyer, J. Appl. Phys. **93**, 8292 (2003).
  - [24] J. P. Liu, C. P. Luo, Y. Liu, and D. J. Sellmyer, Appl. Phys. Lett. **72**, 483 (1998).
  - [25] Y. Gott, M. Ioffe, and V. Tel'kovskii, Nucl. Fusion, 1962 Suppl. **Pt. 3**, 1045 (1962).
  - [26] D. E. Pritchard, Phys. Rev. Lett. **51**, 1336 (1983).
  - [27] T. Bergeman, G. Erez, and H. J. Metcalf, Phys. Rev. A **35**, 1535 (1987).
  - [28] V. Bagnato *et al.*, Phys. Rev. Lett. **58**, 2194 (1987).
  - [29] Y. T. Xing *et al.*, Phys. Stat. Sol. (c) **1**, 3702 (2004).
  - [30] J. Estève *et al.*, Phys. Rev. A **70**, 042629 (2004).
  - [31] D.-W. Wang, M. D. Lukin, and E. Demler, Phys. Rev. Lett. **92**, 076802 (2004).
  - [32] S. Eriksson *et al.*, Appl. Phys. B **79**, 811 (2004).
  - [33] K. Leistner *et al.*, Appl. Phys. Lett. **85**, 3498 (2004).